Journal of Materials Chemistry A

Accepted Manuscript

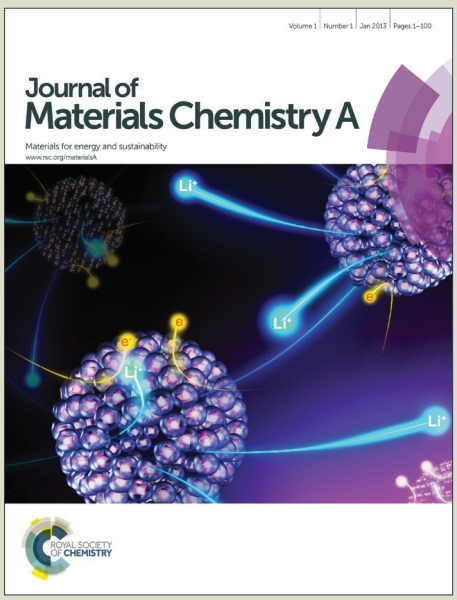

ROYAL SOCIETY OF CHEMISTRY

www.rsc.org/materialsA

SPEEK/Graphene oxide nanocomposite membranes with superior cyclability for high-efficiency vanadium redox flow battery

Wenjing Dai,[a] Yi Shen,[b] Zhaohua Li,[a] Lihong Yu,*[c] Jingyu Xi*[a] and Xinping Qiu*[a,d]

[a] *Lab of Advanced Power Sources, Graduate School at Shenzhen, Tsinghua University, Shenzhen 518055, China. Email: xijingyu@gmail.com; qiuxp@tsinghua.edu.cn.*
[b] *College of Light Industry and Food Sciences, South China University of Technology, Guangzhou, 510640, China.*
[c] *School of Applied Chemistry and Biological Technology, Shenzhen Polytechnic, Shenzhen 518055, China. Email: yulihong@szpt.edu.cn.*
[d] *Key Lab of Organic Optoelectronics and Molecular Engineering, Department of Chemistry, Tsinghua University, Beijing 100084, China.*

Abstract

A series of novel composite membranes based on sulfonated poly(ether ether ketone) (SPEEK) with various graphene oxide (GO) loadings were firstly employed and investigated in vanadium redox flow battery (VRFB). The scanning electron microscopy images of the composite membranes revealed the uniform dispersion of GO nanosheets in the polymer matrix due to the interaction between GO and SPEEK, as confirmed by fourier transform infrared spectra. The mechanical and thermal parameters of the composite membranes increased while the VO^{2+} permeability decreased with GO content increasing. Randomly embedded GO nanosheets in membrane can serve as effective barriers to block the transport of vanadium ion, resulting in significant decrease of vanadium ion permeability. The VRFB assembled with the composite membrane exhibited highly improved cell parameters and strikingly long cycling stability, compared with commercial Nafion 117 membrane. With the protection of porous PTFE substrate, pore filling SPEEK/GO composite membrane based VRFB has run for 1200 cycles with relatively low capacity decline.

1. Introduction

Due to the ever-increasing energy consumption and great concern on environmental effects of fossil fuels, renewable and sustainable energy resources, such as solar and wind energy, have attracted extensive attention in recent years.[1-2] Because of the intermittent and volatile characteristics of solar and wind energy, a low-quality output electricity and mismatch between power generation and demand are inevitable.[3] To address this issue, many efforts have been directed in developing various energy storage technologies, such as redox flow batteries, capacitors and lithium ion batteries.[4-9] In particular, vanadium redox flow battery (VRFB), invented by M. Skyllas-Kazacos,[10] has been considered as a promising technology for large-scale energy storage due to the advantages of long lifespan, fast response time and flexible design.[9-17]

As a key component of VRFB, ion exchange membrane (IEM) is responsible for isolating positive and negative electrolytes to prevent them from cross-mixing while transporting protons and sulfate ions to complete the circuit during charge and discharge processes.[18-20] The performance of VRFB is closely related to the structural properties of the IEM. An ideal IEM should possess high proton conductivity, low vanadium ion permeability, excellent stability and mechanical strength, and low cost.[8,19] Currently, the state-of-the-art Nafion membranes are widely used in VRFB system owing to the excellent proton conductivity and superior chemical stability. However, Nafion membranes also suffer from several drawbacks such as the extremely high cost and low proton/vanadium ion selectivity, which hinder the wide commercialization of VRFB.[18-25]

Up to date, many non-perfluorinated membranes, such as sulfonated poly(ether ether ketone) (SPEEK), sulfonated poly(fluorenyl ether ketone), sulfonated poly(aryl ether sulfone ketone), sulfonated poly(aryl ether sulfone) and sulfonated poly(imide) have been explored to reduce the cost of IEMs in the VRFB systems.[19,26-34] Among these alternatives, SPEEK is considered to be the most attractive candidate to replace Nafion membranes due to its lower cost as well as better ion selectivity as compared with Nafion membranes.[19,26] The properties of SPEEK membranes are highly dependent on the degree of sulfonation (DS). SPEEK membranes with high DS exhibit high proton conductivity and ion exchange capacity (IEC). Meanwhile, the large number of sulfonic acid groups also result in poor mechanical property and high vanadium ion permeability,[35] which is unfavorable for VRFB applications. One remedy for this problem is to incorporate nano-sized inorganic filler materials into SPEEK matrix, such as SiO_2, WO_3 and TiO_2.[26,32,35-37] It was demonstrated that the presence of inorganic fillers could significantly affect the structural

properties of the composite membranes, while the selection of filler and the control of the interaction between the filler and the polymer chains played a decisive role on the performance of the resulting composite IEMs.[26,38]

Recently, graphene oxide (GO) has been of great interest due to its unique two-dimensional layered structure, abundant functional groups, high surface area and intrinsic mechanical stability.[39-45] Various gaphene oxide-based composite IEMs have been successfully employed in proton exchange membrane fuel cells.[46-52] It is expected that the incorporation of GO into SPEEK membranes for VRFB could enhance the performance of the IEMs. The reasons are listed as follows: 1) The two-dimensional layered GO nanosheets can serve as effective barriers to the transport of vanadium ions due to the significant increase in tortuosity; 2) The hydrophilic surface oxygen-containing functional groups of GO are prone to form hydrogen bonds with polymer chains, which is favorable for the formation of the hydrophobic/hydrophilic separation structure in the resulting composite membranes and consequently the enhancement of ion selectivity.[31,47,51] 3) The strong interfacial interaction between GO and the SPEEK membrane host is beneficial for improving the mechanical stability of the pristine SPEEK membranes; 4) The hydrophilic GO possesses good dispersion and could help to retain more water molecules to obtain high IEC in the resulting composite membrane;[53] 5) GO itself can provide proton transport pathway via surface diffusion.[54]

Up to now, few studies have been reported on the application of GO-based composite membranes in VRFB. Herein, we firstly report the preparation and application of a series of SPEEK/GO nanocomposite membranes in VRFB. The resulting SPEEK/GO composite membranes exhibited superior cell performance and cycling stability in VRFB compared with the commercial Nafion 117 membrane. The emphasis was placed on the exploration on the effects of GO on the structural properties of the composite membranes including water uptake, swelling ratio, IEC, proton conductivity, VO^{2+} permeability, ion selectivity, thermal stability, mechanical property and single cell performance.

2. Experimental Section

2.1 Materials

Poly(ether ether ketone) (PEEK) (Victrex, PEEK 450G) was pretreated by washing and then drying at 80 ^{o}C for 24 h in vacuum. Graphene oxide (XF002) was supplied by Nanjing XFNANO Materials Tech Co. Ltd. Nafion 117 membranes were purchased from DuPont Company. Porous PTFE films (thickness of 30 μm and

pore percentage of 80%) were obtained from Shanghai Minglie Chemical Science And Technology Ltd. All the other analytical reagents, including N,N-Dimethylformamide (DMF), H_2SO_4, NaCl, NaOH, $MgSO_4 \cdot 7H_2O$ and $VOSO_4 \cdot 4H_2O$, were purchased from local chemical suppliers and used as received.

2.2 Membrane preparation.

25 g of PEEK was gradually dissolved into 250 mL of H_2SO_4 (98 wt. %) under vigorous mechanical stirring at 50 ^oC for 2.5 h. Afterwards, the polymer solution was slowly poured into excess ice-cold water under continuous agitation to terminate sulfonation reaction. The polymer precipitate was filtered, washed several times with deionized water until the pH reached neutral, and then dried in a vacuum oven at 100 ^oC for 24 h. The DS of synthesized SPEEK was 63% determined by titration method.

The SPEEK/GO composite membranes were prepared using the conventional solution casting method. The details of the procedure are shown as follow. 1.5 g SPEEK was dissolved in 6 mL DMF and a certain amount of GO was dispersed in 4 mL DMF under sonication for 1 h to form a stable suspension. The GO suspension was transferred to the polymer solution under vigorous mechanical stirring for 24 h. The resulting mixture was cast onto flat clean glass. The membranes were dried at 60 ^oC overnight and then at 100 ^oC under vacuum for 12 h. After cooling to room temperature, the SPEEK/GO membranes were peeled off from the glass and soaked in 1 mol/L H_2SO_4 for 24 h. Subsequently, the membranes were immersed into deionized water for 24 h to remove the excess acid and stored in deionized water for further use. To study the effects of the GO content on the properties of the composite membranes, a series of SPEEK/GO composite membranes with 1, 2, 3 and 5 wt. % of GO were prepared. For comparison, pure SPEEK membrane was prepared and treated under the same procedure. Nafion 117 membrane was pretreated according to the literature[26] and used as a reference. The composite membrane is denoted as S/GO X, where X is the weight ratio of GO. For example, S/GO 1 is the composite membrane with 1 wt. % of GO.

Pore filling S/GO 2 composite membrane was fabricated by impregnating the S/GO 2 membrane casting solution into a porous PTFE thin film (denoted as S/GO 2@PTFE). The pure SPEEK membrane was under the same treatment as a comparison (denoted as SPEEK@PTFE).

2.3 Membrane characterization

2.3.1 Membrane Morphology

The morphology of GO nanosheets and membrane cross-sections were observed by a Hitachi S-4800 (Japan) scanning electron microscope (SEM). For viewing the membrane cross-sections, the samples were prepared by fracturing the membranes in liquid nitrogen and subsequently coated with Au.

2.3.2 Fourier transform infrared spectra

Fourier transform infrared spectra (FT-IR) of membranes were recorded on a FT-IR spectrometer (Buker Vertex 70, Germany). The IR spectra were collected after 32 scans between 4000 and 500 cm^{-1} in ATR mode at a resolution of 4 cm^{-1}.

2.3.3 Water uptake and swelling ratio

To evaluate the water uptake and swelling ratio of membranes, membrane samples were firstly soaked in deionized water at room temperature for 24 h, and then wiped with absorbent paper to remove the surface water before measurement. Afterwards, the membranes were dried in vacuum oven at 100 ^{o}C for 24 h. The water uptake and swelling ratio of the membrane were calculated according to the following equations:

$$\text{Water uptake}\ (\%) = \frac{W_w - W_d}{W_d} \times 100\% \quad (1)$$

$$\text{Swelling ratio}\ (\%) = \frac{L_w - L_d}{L_d} \times 100\% \quad (2)$$

where W_w and W_d are the weights of membranes after and before water absorption, respectively; L_w and L_d are the lengths of wet and dry membranes, respectively. Three parallel tests were conducted and the average values were given.

2.3.4 Ion exchange capacity (IEC) and proton conductivity

The ion exchange capability (IEC) of the membrane was measured by traditional titration. Typically, the membranes were first dried and the weights were recorded. Subsequently, the membranes were soaked in 50 mL saturated NaCl solution for 24 h. Afterwards, the solution was back titrated with 0.1 mol/L NaOH. IEC was calculated according to the following equation:

$$\text{IEC}\,(\text{mmol}/\text{g}) = \frac{C_{NaOH} \times V_{NaOH}}{W_d} \quad (3)$$

where V_{NaOH} is the consumed volume of NaOH solution and C_{NaOH} is the concentration of NaOH solution.

The proton conductivity of sample membranes was measured by electrochemical impedance spectroscopy (EIS) using a PARSTAT 2273 electrochemical station (USA, AMETEK, Inc.). The proton conductivity (σ) was calculated according to the following equation:

$$\sigma = \frac{d}{RS} \quad (4)$$

where S and d are the area and thickness of the membrane, and R is the impedance. Three repeated measurements were conducted for each parameter and the averages of three testing values were recorded.

2.3.5 Permeability of VO^{2+} and selectivity

The VO^{2+} permeability through the membrane was measured with the method described in the reference.[26] The membrane was sandwiched between two diffusion half cells. The left reservoir was filled with 1.5 mol/L $VOSO_4$ in 3 mol/L H_2SO_4 solution and the right one was filled with 1.5 mol/L $MgSO_4$ in 3 mol/L H_2SO_4 solution. The two solutions were continuously magnetically stirred to avoid the concentration polarization. The effective area of the membrane was 7 cm^2 and the added volume of solutions in the half-cells was 40 mL. The concentration of VO^{2+} in the left reservoir was monitored as a function of time using a Spectrum lab 752S UV–Vis spectrophotometer (China, Leng Guang Tech.). The ion selectivity of membrane is defined as the ratio of the proton conductivity and the VO^{2+} permeability.

2.3.6 Mechanical properties and thermal analysis

Tensile measurements on the samples were carried out using a universal test machine (SANS, CMT-4204, China) with a programmed elongation rate of 2 mm/min under 20 ± 2 °C and 50% relative humidity. The samples were cut into dumbbell shape with a width of 3.5 mm in the narrow region. For each membrane, three measurements were conducted and the average value was recorded. The thermal properties of the membranes were characterized by a thermal gravimetric analyzer (Perkin Elmer Pyris 1 TGA), heated from 100 °C to 750 °C at a rate of 10 °C/min under nitrogen atmosphere.

2.4 VRFB single cell performance

The VRFB single cell was assembled by sandwiching a membrane (70 mm × 70 mm) with two graphite felt electrode (50 mm × 50 mm × 5 mm), and two graphite polar plates (60 mm × 60 mm × 3 mm) served as current collectors.[26] Two 50 mL of 2 mol/L VO^{2+}/V^{3+} (mol/mol = 1:1) in 2 mol/L H_2SO_4 solution, serving as the starting negative and positive electrolytes, were cycled using peristaltic pumps (BT00-300T) with a flow rate of 60 mL/min. The cell was charged and discharged using a battery testing system (CT-3008W-5V6A, Neware). The upper limit of charge voltage and the lower limit of discharge voltage were 1.65 V and 0.8 V, respectively. The digital photo of some VRFB single cells was shown in Scheme 1. For the single cell efficiency, 5 cycles at each current density were run and the average values were given.

3. Results and discussion

3.1 Membrane preparation and morphology

The preparation procedure of SPEEK membrane from commercial PEEK granules is shown in Scheme 1. This procedure is simple and controllable, allowing large-scale production of the cost-effective SPEEK membranes. The SEM images of GO nanosheets and the composite membranes are investigated as shown in Fig. 1. GO nanosheets show some wrinkles at high magnification (Fig. 1a), consistent with the typical morphology of GO nanosheets.[38,47] From Fig. 1(b) to (d), the cross-sectional SEM images of SPEEK, S/GO 2 and S/GO 3 composite membranes are compared to examine the microstructure of the SPEEK membrane after incorporating GO nanosheets. It is observed that the pure SPEEK membrane has a relatively smoother cross section, while the S/GO composite membranes display rougher cross sections. It is also seen that GO nanosheets are uniformly dispersed into the SPEEK matrix and tightly bound at the interface due to the favorable interaction between GO and the SPEEK matrix. Increasing GO loading, the S/GO composite membranes maintain uniform and translucent, with color changing from yellow to brown as shown in the digital photos (insets in Fig. 1(b), (c) and (d)).

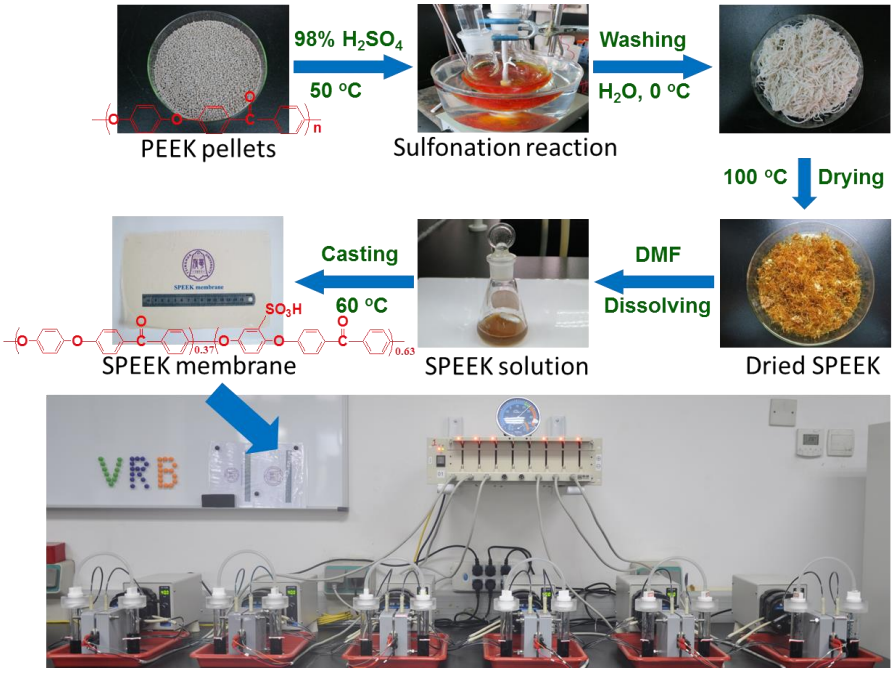

Scheme 1 Preparation procedure of SPEEK membrane and digital photo of VRFB single cells during charge-discharge test.

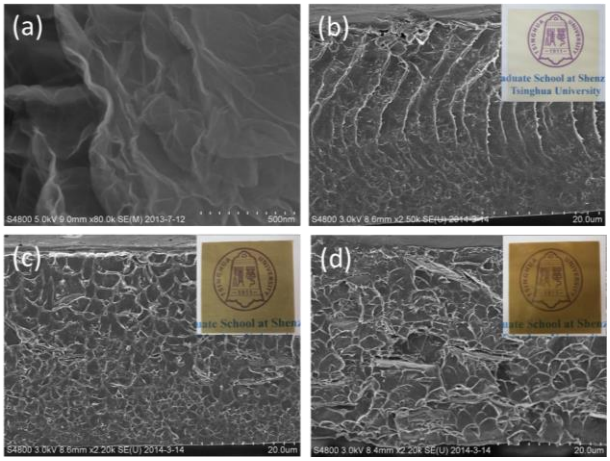

Fig. 1 SEM images of (a) GO nanosheets, and cross-sections of (b) SPEEK, (c) S/GO 2 and (d) S/GO 3 membranes. The insets in (b), (c) and (d) are the corresponding digital photos of the membranes. The bar in (a) is 500 nm while those in (b), (c) and (d) are 20 µm.

3.2 Fourier transform infrared spectra

There are abundant oxygen-containing groups such as carbonyl (C=O), hydroxyl (-OH), carboxyl (-COOH) as well as oxygen epoxide groups (bridging oxygen atoms) at both sides of GO,[53] and therefore the interfacial interaction between GO and SPEEK matrix should be verified. Fig. 2 shows the FT-IR spectra of SPEEK and S/GO 2 membranes over the range of 4000-500 cm^{-1}. The SPEEK membrane shows a peak at 3440 cm^{-1} arising from the presence of –OH (from $–SO_3H$), while S/GO 2 membrane shows a characteristic intermolecular hydrogen bond broad peak at 3445 cm^{-1} arising from –OH on the GO surface and also from $–SO_3H$. For SPEEK membrane, the bands at 1286 cm^{-1} and 1083 cm^{-1} are associated with asymmetric and symmetric stretching vibrations of the O=S=O group, while for S/GO 2 membrane, the corresponding bands are shifted to 1280 cm^{-1} and 1070 cm^{-1} due to the interaction between GO with SPEEK. The peak assignments are according to literature reported values.[38,47] The results clearly indicate the formation of hydrogen bonds between the sulfonated acid groups in SPEEK and polar groups (-OH, -COOH) on GO, which may be beneficial for the improvement of mechanical stability.

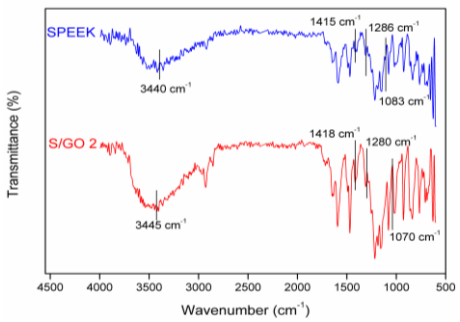

Fig. 2 FT-IR spectra of SPEEK and S/GO 2 membranes.

3.3 Physicochemical properties

The physicochemical properties, VO^{2+} permeability and selectivity of all membranes are listed in Table 1. The SPEEK and S/GO membranes are all controlled to be 50–60 μm thick, which are much thinner than Nafion 117 membrane (220 μm). As shown in Table 1, the water uptake, swelling ratio and IEC of the composite membranes increase with the GO content, owing to the hydrophilic nature of GO. This implies that even with very small amount of fillers, GO can effectively enhance the hydrophilicity of SPEEK and facilitate the absorption and retention of water molecules. On the other hand, the proton conductivity of the S/GO composite membranes decreases with the GO loading. This is related to the blocking effect of the GO filler, explained as follows: although high water uptake can facilitate proton migration[55] and GO itself can provide proton transport pathway via surface diffusion[54], the blocking effect of proton-nonconductive GO nanosheets with large surface plays a dominant role in the proton conductivity of the composite membranes. Nevertheless, the S/GO composite membranes illustrate excellent VRFB cell performance in spite of the lower proton conductivity compared to Nafion 117 membrane, as verified by the following results.

Table 1 Physicochemical properties, vanadium ion permeability and selectivity of the membranes.

Samples	Thickness (μm)	Water uptake (%)	Swelling ratio (%)	IEC (mmol/g)	Proton conductivity (mS/cm)	Vanadium permeability (10^{-7} cm^2/min)	Selectivity (10^4 S min/cm^3)
Nafion 117	220	33.0	18.6	0.80	31.9	34.9	0.91
SPEEK	52	37.1	8.0	1.85	16.9	11.5	1.47
S/GO 1	55	40.1	10.6	1.98	15.3	9.2	1.66
S/GO 2	52	42.6	11.7	2.04	14.9	7.9	1.88
S/GO 3	50	44.9	12.5	2.07	10.2	5.9	1.74
S/GO 5	58	47.1	14.4	2.13	7.5	5.2	1.44
SPEEK@PTFE	63	36.5	7.2	1.77	16.4	11.1	1.48
S/GO 2@PTFE	67	41.6	11.1	2.00	14.6	7.6	1.92

3.4 Permeability of VO^{2+} and selectivity

The VO^{2+} permeability of SPEEK membrane is much lower than that of Nafion 117 membrane (11.5 × 10^{-7} cm^2/min vs 34.9 × 10^{-7} cm^2/min), as shown in Table 1. This is due to their different microstructures. The microstructure of SPEEK membrane has smaller hydrophobic/hydrophilic separation (the backbone is less hydrophobic and the sulfonic acid group is less acidic) compared to Nafion polymer.[26,48] Thus, the

separation of the hydrophobic and hydrophilic domain is less pronounced, which leads to lower vanadium ion permeability than that of Nafion 117. A linear relationship between the concentration change of VO^{2+} and time is clearly illustrated in Fig. 3. The slope of each line can reflect the VO^{2+} permeability value of the corresponding membrane. It is found that the VO^{2+} permeability across the composite membranes decreases with the GO content, which can be also seen from Table 1. On one hand, the impermeable two-dimensional layered GO nanosheets can serve as effective barriers to prevent vanadium ions from migrating through the membrane due to the significant increase in tortuosity as shown in Scheme 2 (the left part). This blocking effect of GO nanosheets in the membrane leads to a decreasing trend in vanadium ions permeability. On the other hand, the interfacial interaction between GO and SPEEK matrix can restrict the formation of hydrophilic channels[48] used for the transport of vanadium ions, which can also contribute to the decrease of vanadium ions permeability as shown in the right part of Scheme 2.

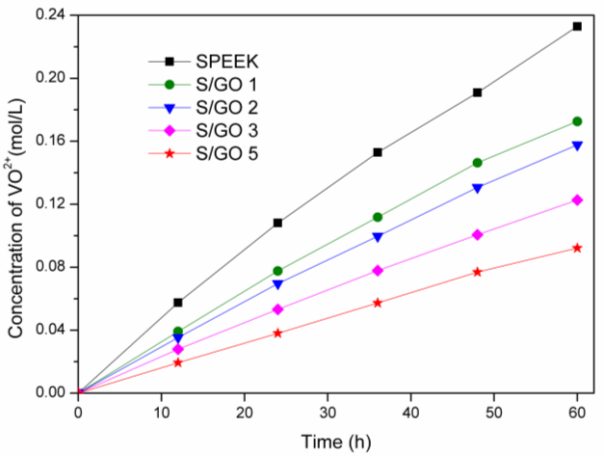

Fig. 3 Concentration change of VO^{2+} in $MgSO_4$ solution across SPEEK and S/GO membranes.

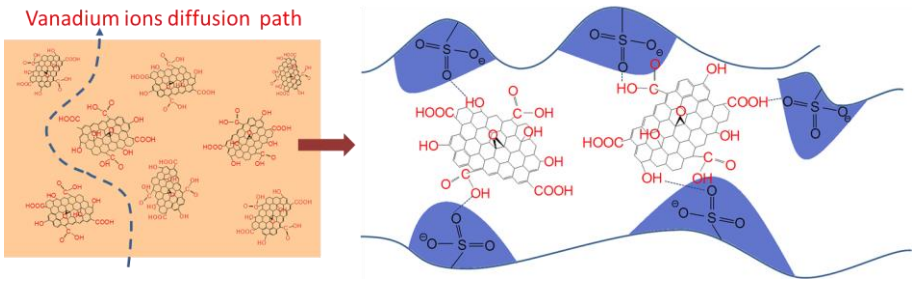

Scheme 2 The mechanism of blocking vanadium ion migration in S/GO composite membrane.

The selectivity is a comprehensive factor for evaluating membrane performance, which is defined as the ratio of proton conductivity and vanadium ion permeability. Generally a higher selectivity value implies

better performance in VRFB.[26] From Table 1, the S/GO 2 membrane shows a much higher selectivity of 1.88 ×10^4 S min/cm^3, about two times that of Nafion 117 membrane (0.91 ×10^4 S min/cm^3).

Fig. 4 shows the VO^{2+} permeability and selectivity of Nafion 117, SPEEK and S/GO membranes. The S/GO 2 and S/GO 3 composite membranes exhibit comparatively higher selectivity among all the composite membranes. It is expected that the VRFB assembled with the two membranes will show better cell performance. Therefore, the following investigations are directed at these two kinds of composite membranes in comparison with Nafion 117 and the pristine SPEEK membranes.

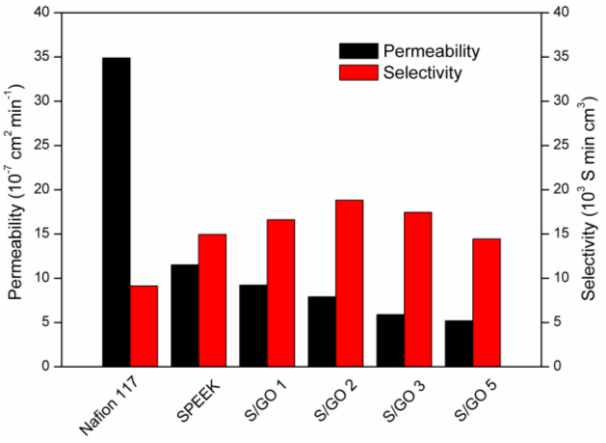

Fig. 4 VO^{2+} permeability and selectivity of Nafion 117, SPEEK and S/GO membranes.

3.5 Mechanical properties and thermal analysis

The mechanical properties of composite membranes could be improved by the incorporation of inorganic fillers.[56] The mechanical properties of Nafion 117, SPEEK, S/GO 2 and S/GO 3 membranes are presented in Table 2. The breaking strength of the S/GO composite membranes increases with the GO content. The pure SPEEK membrane has the lowest breaking strength due to the high DS. The percentage elongation of the pure SPEEK and S/GO composite membranes is between 82%-86%, which is much smaller than that of Nafion 117 (218%). The result indicates that the incorporation of GO nanosheets into SPEEK matrix can enhance the mechanical strength of the composite membrane owing to the strong hydrogen bonds interaction between GO and SPEEK (scheme 2), as confirmed by the aforementioned FTIR results. On the whole, S/GO 2 and S/GO 3 membranes exhibit better mechanical properties than pure SPEEK and Nafion 117 membranes, which are tough enough to be used as IEMs for VRFB.

Table 2 Mechanical properties of the membranes.

Samples	Breaking strength (MPa)	Percentage elongation (%)
Nafion117	21.4	218
SPEEK	16.7	86
S/GO 2	28.2	83
S/GO 3	31.4	82

The thermal properties of SPEEK and the S/GO composite membranes are compared to evaluate the effect of GO incorporation. As shown in Fig. 5, the thermal decomposition of all the samples occurs in two stages. The first stage (290 °C – 330 °C) is attributed to the degradation of sulfonic acid group of SPEEK; The second stage (400 °C – 550 °C) is assigned to the decomposition of the SPEEK backbone.[26] As the content of GO increases, the TGA curves shift slightly toward higher temperatures, suggesting a higher thermal stability of the S/GO composite membranes compared to pure SPEEK membrane due to the interaction between GO and SPEEK.[57] The thermal analysis results are consistent with FT-IR and mechanical test.

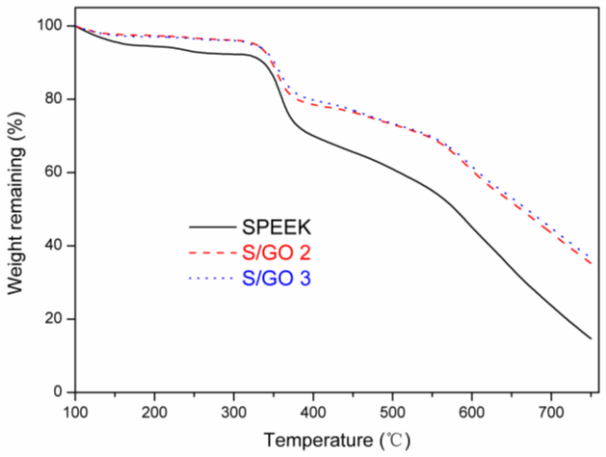

Fig. 5 TGA curves of SPEEK, S/GO 2 and S/GO 3 membranes.

3.6 VRFB single cell performance

Since S/GO 2 and S/GO 3 composite membranes have superior properties based on all the above results, we choose them to assemble VRFB for further investigation in comparison with Nafion 117 and SPEEK membranes. Fig. 6 represents the charge–discharge curves of VRFBs based on Nafion 117, SPEEK, S/GO 2 and S/GO 3 membranes, obtained at the current densities of 80, 120, 160 and 200 mA/cm^2, respectively. The charge and discharge capacity for membranes demonstrates a trend of S/GO 3 > S/GO

2 > SPEEK > Nafion 117 at all current densities and the gap between them is widening with the increase of current density. S/GO 2 and S/GO 3 membranes show similarly outstanding curves at all current densities, indicating that S/GO composite membranes possess excellent properties to restrict the cross-mixing of vanadium ions and thus the capacity loss by self–discharge can be suppressed. The VRFBs with S/GO composite membranes show lower charge voltage platform and higher discharge voltage platform than those with Nafion 117 and SPEEK membranes. This is assigned to the good balance of proton conductivity and vanadium ion permeability in composite membranes.

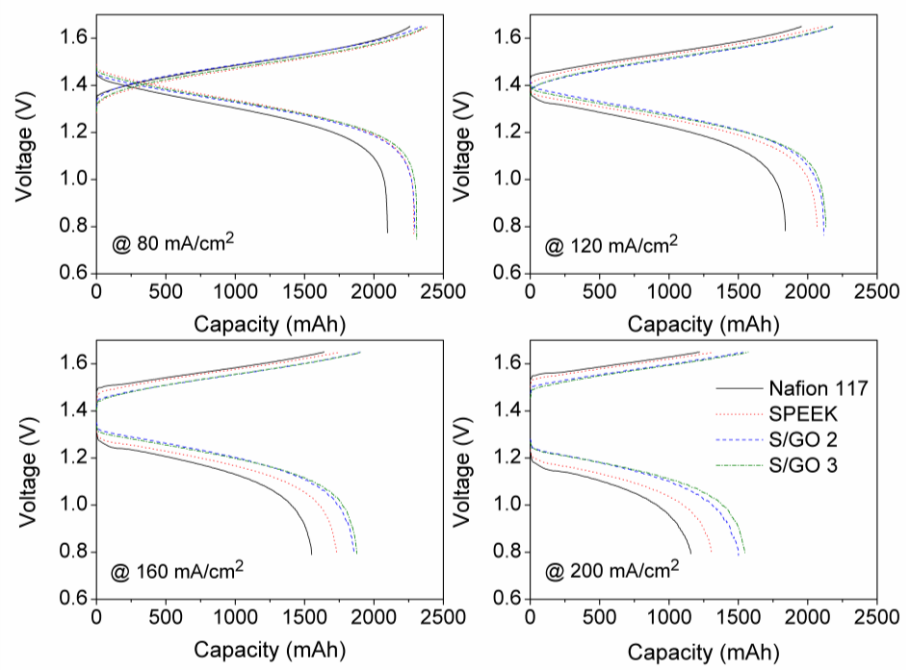

Fig. 6 Charge-discharge curves of VRFBs with Nafion 117, SPEEK, S/GO 2 and S/GO 3 membranes at 80, 120, 160 and 200 mA/cm^2.

The relationships of coulombic efficiency (CE), voltage efficiency (VE) and energy efficiency (EE) with charge–discharge current densities from 40 to 200 mA/cm^2 are illustrated in Fig. 7. The CE for different membranes has an order of S/GO 3 > S/GO 2 > SPEEK > Nafion 117 at 40–120 mA/cm^2, in accordance with the result of VO^{2+} permeability. However, the CE of S/GO 2-VRFB exceeds that of S/GO 3-VRFB at 140–200 mA/cm^2, suggesting that S/GO 2 has certain advantage in the high current density charge–discharge process. At 80 mA/cm^2, the CE of S/GO 2-VRFB is 96.9%, much higher than that (92.8%) of Nafion 117-VRFB owing to the lower VO^{2+} permeability. The VE has a rank of S/GO 3 > S/GO 2 > SPEEK > Nafion 117 at all current densities, in good agreement with the results of the charge–discharge curves in Fig. 6.

The EE of VRFBs with two S/GO composite membranes is higher than that of VRFBs with Nafion 117 and SPEEK membranes at all current densities due to the better selectivity as discussed above. At 80 mA/cm^2, the EE of S/GO 2-VRFB is 84.2%, while the EE of Nafion 117-VRFB is just 79.5%. On the whole, the remarkable improvement of the cell efficiency can be mainly attributed to the excellent performance of S/GO composite membranes to suppress the cross-mixing of vanadium ions.

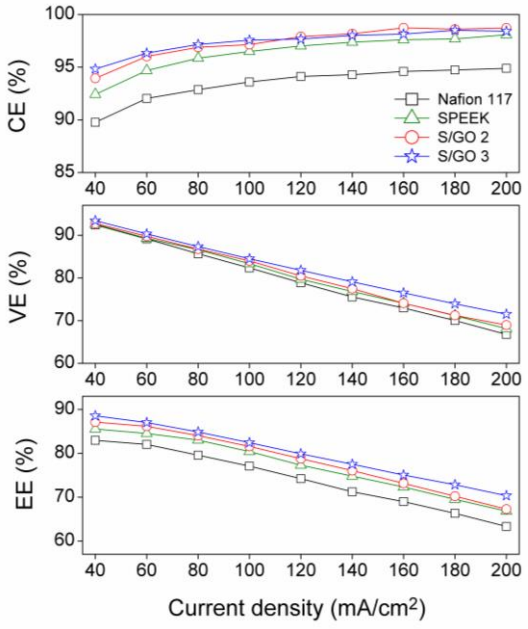

Fig. 7 Cell performance of VRFBs with Nafion 117, SPEEK, S/GO 2 and S/GO 3 membranes under different current densities.

To further investigate the stability of S/GO composite membranes in VRFB under strong oxidizing and acidic condition, the VRFBs assembled with all the aforementioned membranes were run continuously until the discharge capacity retention became low. The discharge capacity decline is owing to the unbalanced transports of vanadium ions and water, accompanied with some side reactions.[26] The detailed cycle performance of the VRFBs over 300 cycles at 80 mA/cm^2 is shown in Fig. 8. It can be seen that pure SPEEK membrane ruptures at the 67th cycle due to its poor mechanical property and chemical stability caused by the high DS. As presented, the CEs of the cells with Nafion 117, S/GO 2, and S/GO 3 membranes all remain nearly constant during the whole 300 cycles, while the capacity retentions of the cells with Nafion 117, S/GO 2, and S/GO 3 membranes are 16.2%, 50.1% and 37.9%, respectively, after 300 cycles. It can be concluded that S/GO 2 composite membrane possesses a superior chemical stability in vanadium solutions under strong oxidizing and acidic conditions.

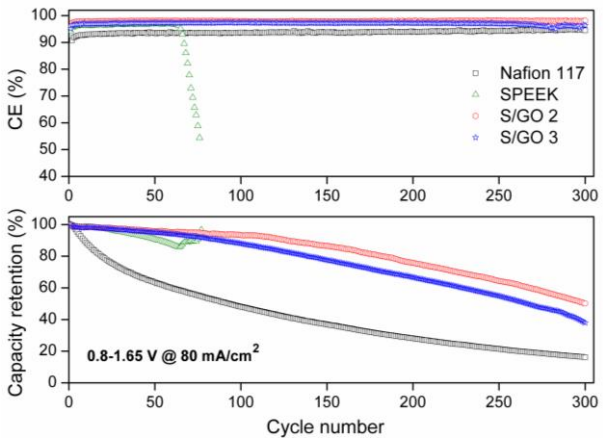

Fig. 8 Cycle performance of VRFBs with Nafion 117, SPEEK, S/GO 2 and S/GO 3 membranes.

The charge–discharge curves for VRFBs with Nafion 117 and S/GO 2 membranes over 200 cycles are compared in Fig. 9. The change in charge–discharge voltage platform of S/GO 2-VRFB is smaller and the capacity loss of S/GO 2-VRFB is less than those of Nafion 117-VRFB over 200 cycles, indicating a lower vanadium ions permeation through S/GO 2 membrane. The above cycling results confirm that the introduction of GO nanosheets into SPEEK membrane can greatly enhance the cycling stability of S/GO composite membranes.

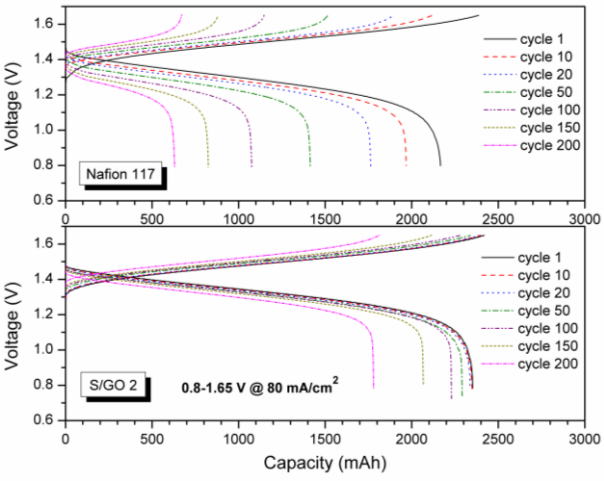

Fig. 9 Charge-discharge curves for VRFBs with Nafion 117 and S/GO 2 membranes over 200 cycles.

The SEM images of membranes after long cycling test are shown in Fig. 10. The cross sections of the S/GO composite membranes after long cycling test show no obvious changes as compared with those of the fresh membranes(see Fig. 1), indicating the outstanding stability of the composite membranes.

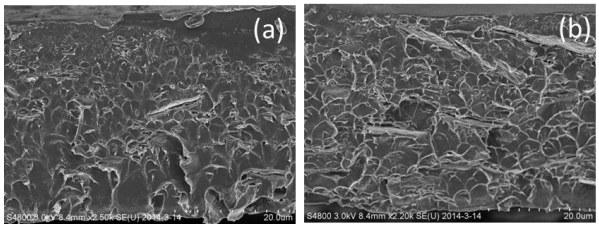

Fig. 10 Cross-section SEM images of the composite membrane after 300 cycles charge-discharge test. (a) S/GO 2 and (b) S/GO 3. The bars are both 20 μm.

Pore filling membranes technology is an effective method to improve the chemical stability of IEMs, which have been successfully used in fuel cells.[58-62] Highly stable polymer, such as poly(tetrafluoroethylene) (PTFE) and polyethylene (PE), are often used as the porous substrate of pore filling membranes. In this study, to further improve the cycling stability of S/GO composite membranes for application in long–life VRFB systems, we selected S/GO 2 membrane and fabricated a pore filling membrane (denoted as S/GO 2@PTFE). The pure SPEEK membrane was under the same treatment as a comparison (denoted as SPEEK@PTFE). Surface SEM image of porous PTFE film and the digital photos of porous PTFE film and the pore filling membranes are shown in Fig. 11. Porous PTFE film is white and translucent in appearance (Fig. 11a), and PTFE is a robust host with highly porous structure (Fig. 11b), which can contribute to improve the mechanical strength and chemical stability of the resulting pore filling membranes.[62,63] From Fig. 11 (c) and (d), we can see the resulting pore filling membranes are both homogeneous and have the same color as the pristine membranes (Fig. 1).

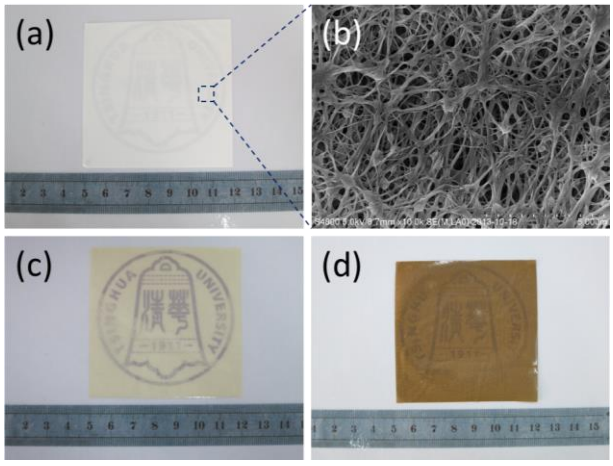

Fig. 11 Surface SEM image of porous PTFE membrane (b); the bar is 5μm. Digital photos of PTFE film (a), SPEEK@PTFE membrane (c) and S/GO 2@PTFE membrane (d).

As shown in Table 1, only slight changes are observed in the properties of the resulting pore filling membranes as compared with the standard membranes. The resulting pore filling membranes become thicker than the standard membranes of each type. The water uptake, swelling ratio and IEC of the pore filling membrane are slightly lower than those of the corresponding standard membrane due to the poor hydrophilicity of PTFE substrate. Compared with the standard membrane, both the proton conductivity and the vanadium permeability of the resulting pore filling membrane decrease, resulting in a maximum selectivity of 1.92 $\times 10^4$ S min/cm^3 in the S/GO 2@PTFE membrane. It is worth noting that the selectivity of the S/GO 2@PTFE membrane is more than two times that of Nafion 117 membrane (0.91 $\times 10^4$ S min/cm^3).

The cell performance and cycle life test of VRFBs with the resulting pore filling membranes are also conducted at 80 mA/cm^2 for comparison. The CE, VE, EE of S/GO 2-VRFB are 96.9%, 86.7% and 84.0%, separately; while the CE, VE, EE of S/GO 2@PTFE-VRFB are 98.4%, 82.5% and 81.2%, respectively, which is in accordance with the results of the vanadium permeability and the proton conductivity. The CE of VRFB assembled with the pore filling membrane increases due to the lower vanadium permeability, while the lower proton conductivity of the pore filling membrane is responsible for the decreased VE and EE of VRFB.

The detailed results of cycle life test are shown in Fig. 12. The CE and EE of the VRFBs with SPEEK@PTFE and S/GO 2@PTFE membranes all show no obvious decline. From Fig. 8, we can see that the capacity retention of S/GO 2-VRFB is 50.1% at 300 cycles, and the pure SPEEK membrane ruptures at 67 cycles. In contrast, at 300 cycles, the capacity retention of S/GO 2@PTFE-VRFB is 78.7%, which is more than twice that (36.3%) of SPEEK@PTFE-VRFB. In addition, the capacity of the VRFB with S/GO 2@PTFE membrane still remain 30.4% of the origin capacity after 1200 cycles, much higher than that (13.2%) with SPEEK@PTFE membrane after 500 cycles. To the best of our knowledge, this is the first report that SPEEK-based membrane can be successfully used in VRFB for more than 1000 charge–discharge cycles at a current density of 80 mA/cm^2 in 2 mol/L vanadium electrolyte.

Fig. 13 is a comparison chart of the capacity retention rate of VRFBs with Nafion 117, S/GO 2, S/GO 3 and S/GO 2@PTFE membranes as a function of cycle number at 80 mA/cm^2. As shown in Fig. 13, when the capacity retention decays to 90%, the cycle number of the VRFB with Nafion 117 membrane is only 8; and the cycle number of the VRFBs with S/GO 2 and S/GO 3 membranes are 128 and 90, respectively; whereas the cycle number of S/GO 2@PTFE membrane is actually 214. When the capacity retention decays to 70%, the VRFBs with Nafion 117, S/GO 2, S/GO 3 and S/GO 2@PTFE membranes are run for 28, 221, 186 and

450 cycles, respectively; And when the capacity retention reaches 50%, the VRFBs with Nafion 117, S/GO 2, S/GO 3 and S/GO 2@PTFE membranes are run for 77, 295, 267 and 1087 cycles, respectively. By comparing the change of the cycle number with the capacity retention of the VRFBs with each membrane, we can conclude that the incorporation of GO greatly enhances the cycling stability of S/GO composite membranes and PTFE can effectively reinforce S/GO composite membranes and further prolong the life time of S/GO composite membranes for long-life VRFB application.

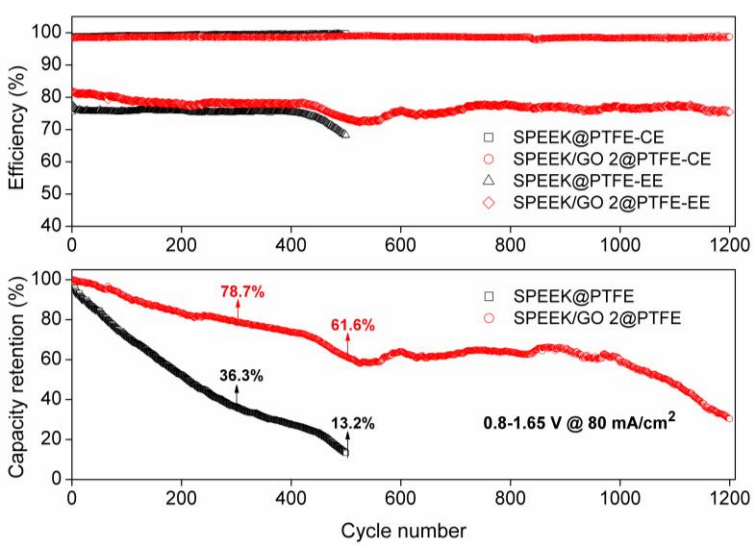

Fig. 12 Cycle performance of VRFBs with SPEEK@PTFE membrane and S/GO 2@PTFE membrane.

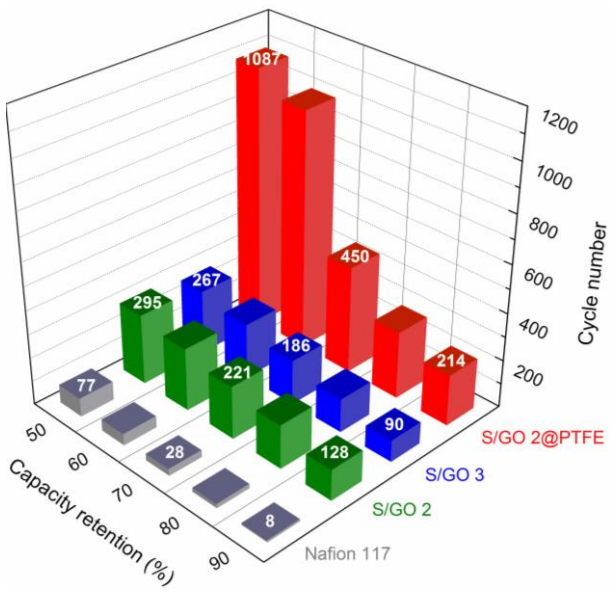

Fig. 13 The comparison chart of the capacity retention rate of VRFBs with Nafion 117, S/GO 2, S/GO 3 and S/GO 2@PTFE membranes as a function of cycle number. (Current density: 80 mA/cm^2)

4. Conclusions

A series of SPEEK/GO composite membranes were fabricated and successfully used in VRFB. The uniform dispersed GO nanosheets in SPEEK matrix act as a physical barrier to prevent the vanadium ions from cross-mixing, resulting in lower vanadium ion permeability and higher ion selectivity. The hydrogen bonding interaction between GO filler and SPEEK matrix is beneficial for the improvement of mechanical stability. Therefore, higher cell efficiency and superior cycling stability are obtained for VRFB with the S/GO composite membrane as compared with the commerical Nafion 117 membrane. To further prolong the cycle stability of the SPEEK/GO composite membrane for long-life VRFB application, a PTFE-based pore filling membrane was fabricated. Strikingly, the VRFB with the resulting pore filling membrane SPEEK/GO@PTFE has run for up to 1200 cycles with a very stable CE (~99%) and relatively low capacity decline, indicating that the low-cost PTFE reinforced SPEEK/GO composite membrane has great potential for usage in high-efficiency and long-life VRFB system.

Acknowledgements

This work was supported by the National Basic Research Program of China (2009CB220105, 2013CB934000), National Natural Science Foundation of China (21273129, 20973099), Shenzhen Science Fund for Distinguished Young Scholars (JC201104210149A) and Shenzhen Basic Research Project (CXZZ20130322164607310, JCYJ20130402145002403, and JCYJ20120830152316442).

Notes and references

1 B. Dunn, H. Kamath and J. Tarascon, *Science*, 2011, **334**, 928.

2 S. Chu and A. Majumdar, *Nature*, 2012, **488**, 294.

3 W. Wang, Q.T. Luo, B. Li, X.L. Wei, L.Y. Li and Z.G. Yang, *Adv. Funct. Mater.*, 2013, **23**, 970.

4 J. Liu, J. Zhang, Z. Yang, J.P. Lemmon, C. Imhoff, G.L. Graff, L. Li, J. Hu, C. Wang, J. Xiao, G. Xia, V.V. Viswanathan, S. Baskaran, V. Sprenkle, X. Li, Y. Shao and B. Schwenzer, *Adv. Funct. Mater.*, 2013, **23**, 929.

5 W. A. Braff, M. Z. Bazant and C. R. Buie, *Nat. Commun.*, 2013, **4**, 2346

6 B. Huskinson, M. P. Marshak, C. Suh, S. Er, M. R. Gerhardt, C. J. Galvin, X. Chen, A. Aspuru-Guzik, R. G. Gordon and M. J. Aziz, *Nature*, 2014, **505**, 195.

7 M. Skyllas-Kazacos, M. H. Chakrabarti, S. A. Hajimolana, F. S. Mjalli and M. Saleem, *J. Electrochem. Soc.*, 2011, **158**, 55.

8 B. Schwenzer, J. L. Zhang, S. Kim, L. Y. Li, J. Liu and Z. G. Yang, *ChemSusChem*, 2011, **4**, 1388.

9 C. Ding, H. M. Zhang, X.F. Li, T. Liu and F. Xing, *J. Phys. Chem. Lett.*, 2013, **4**, 1281.

10 M. Skyllas-Kazacos, M. Rychcik, R.G. Robins, A.G. Fane and M.A. Green, *J. Electrochem. Soc.*, 1986, **133**, 1057.

11 Z. Yang, J. Zhang, M.C.W. Kintner-Meyer, X. Lu, D. Choi, J.P. Lemmon and J. Liu, *Chem. Rev.*, 2011, **111**, 3577.

12 P. K. Leung, X. Li, C. Ponce de Léon, L. Berlouis, C.T.J. Low and F.C. Walsh, *RSC Adv.* 2012, **2**, 10125.

13 G. Kear, A. A. Shah and F. C. Walsh, *Int. J. Energy Res.*, 2011, **36**, 1105.

14 W. Zhang, J. Xi, Z. Li, H. Zhou, L. Liu, Z. Wu and X. Qiu, *Electrochim. Acta*, 2013, **89**, 429.

15 J. Xi, W. Zhang, Z. Li, H. Zhou, L. Liu, Z. Wu and X. Qiu, *Int. J. Electrochem. Sci.,* 2013, **8**, 4700.

16 L. Liu, J. Xi, Z. Wu, W. Zhang, Z. Li, H. Zhou, W. Li and X. Qiu, *J. Appl Electrochem*., 2012, **42**,1025.

17 S. T. Senthilkumar, R. Selvan, N. Ponpandian, J. S. Melo and Y. S. Lee, *J. Mater. Chem. A*, 2013, **1**, 7913.

18 H. Prifti, A. Parasuraman, S. Winardi, T. M. Lim and M. Skyllas-Kazacos, *Membranes*, 2012, **2**, 275.

19 X. Li, H. Zhang, Z. Mai, H. Zhang and I. Vankelecom, *Energy Environ. Sci.*, 2011, **4**, 1147.

20 J. Y. Xi, Z. H. Wu, X. G Teng, Y. T. Zhao, L. Q. Chen and X. P. Qiu, *J. Mater. Chem.*, 2008, **18**, 1232.

21 J. Zeng, C. P. Jiang, Y. H. Wang, J. W. Chen, S. F. Zhu, B. J. Zhao and R. Wang, *Electrochem. Commun*., 2008, **10**, 372.

22 X. G. Teng, Y. T. Zhao, J. Y. Xi, Z. H. Wu, X. P. Qiu and L. Q. Chen, *J. Membrane Sci.*, 2009, **341**, 149.

23 J. Y. Xi, Z. H. Wu, X. P. Qiu and L. Q. Chen, *J. Power Sources*, 2007, **166**, 531.

24 N. Wang, S. Peng, D. Lu, S. Liu, Y. Liu and K. Huang, *J. Solid State Electrochem.*, 2012, **4**, 1577.

25 X. G. Teng, Y. T. Zhao, J. Y. Xi, Z. H. Wu, X. P. Qiu and L. Q. Chen, *J. Power Sources*, 2009, **189**, 1240.

26 Z. Li, W. Dai, L. Yu, J Xi, X. Qiu and L. Chen, *J. Power Sources*, 2014, **257**, 221.

27 S. Kim, J. Yan, B. Schwenzer, J. Zhang, L. Li, J. Liu, Z. Yang and M. A. Hickner, *Electrochem. Commun.*, 2010, **12**, 1650.

28 Z. Mai, H. Zhang, X. Li, C. Bi and H. Dai, *J. Power Sources*, 2011, **196**, 482.

29 W. Dai, L. Yu, Z. Li, J. Yan, L. Liu, J. Xi and X. Qiu, Electrochim. Acta, 2014, **132**, 200.

30 D. Chen, S. Wang, M. Xiao and Y. Meng, *Energy Environ. Sci.*, 2010, **3,** 622.

31 Z. Li, J. Xi, H. Zhou, L. Liu, Z. Wu, X. Qiu and L. Chen, *J. Power Sources*, 2013, **237**, 132.

32 N. Wang, S. Peng, H. Wang, Y. Li, S. Q. Liu and Y. Liu, *Electrochem. Commun.*, 2012, **17**, 30.

33 S. Zhang, B. Zhang, D. Xing and X. Jian, *J. Mater. Chem. A*, 2013, **1**, 12246.

34 M. J. Jung, J. Parrondo, C. G. Arges and V. Ramani, *J. Mater. Chem. A*, 2013, **1**, 10458.

35 S. Molla and V. Compan, *Int. J. Hydrogen Energy*, 2014, **39**, 5121.

36 H. Zhang and P. Shen, *Chem. Rev*., 2012, **112**, 2780.

37 C. Laberty-Robert, K. Valle, F. Pereira and C. Sanchez, *Chem. Soc. Rev*., 2011, **40**, 961.

38 R. Kumar, M. Mamlouk and K. Scott, *RSC Adv*., 2014, **4**, 617.

39 D. R. Dreyer, S. Park, C. W. Bielawski and R. S. Ruoff, *Chem. Soc. Rev.*, 2010, **39,** 228.

40 O. C. Compton and S. T. Nguyen, *Small,* 2010, **6**, 711.

41 Y. W. Zhu, S. Murali, W. W. Cai and X.S. Li, et al, *Adv. Mater.*, 2010, **22**,3906.

42 P. Han, H. Wang, Z. Liu, X. Chen, W. Ma, J. Yao, Y. Zhu and G. L. Cui, *Carbon*, 2011, **49**, 693.

43 J. C. Shearer, A. Cherevan and D. Eder, *Adv. Mater.*, 2014, **26**, 2295.

44 K. S. Novoselov, V. I. Fal`ko, L. Colombo, P. R. Gellert, M. G. Schwab and K. Kim, *Nature*, 2012, **490**, 192.

45 Y. Q. Sun and G. Q. Shi, *J. Polym. Sci. Pol. Phys*., 2013, **51**, 231.

46 B. G. Choi, Y. S. Huh, Y. C. Park, D. H. Jung, W. H. Hong, H. S. Park, *Carbon*, 2012, **50**, 5395.

47 H. Zarrin, D. Higgins, Y. Jun, Z. W. Chenq and M. Flowler, *J. Phys. Chem. C*, 2011, **115**, 20774.

48 Y. S. Heo, H. Im and J. Kim, *J. Membrane Sci*., 2013, **425**, 11.

49 C. Xu, Y. Cao, R. Kumar, X. Wu, X. Wang and K. Scott, *J. Mater. Chem.*, 2011, **21**, 11359.

50 Y. S. Ye, C. Y. Tseng, W. C. Shen, J. S. Wang, K. J. Chen, M. Y. Cheng, J. Rick, Y. J. Huang, F. C. Chang and B. J. Hwang, *J. Mater. Chem.*, 2011, **21**, 10448.

51 Y. C. Cao, C. Xu, X. Wu, X. Wang, L. Xing and K. Scott, *J. Power Sources*, 2011, **196**, 8377.

52 L. Y. Zhang, T. J. Shi, S .L. Wu and H. O. Zhou, *Colloid. Polym. Sci.*, 2013, **291**, 2061.

53 Z. Q. Jiang, X. S. Zhao and A. Manthiram, *Int. J. Hydrogen Energy*, 2013, **38**, 5875.

54 M. R. Karim, K. Hatakeyama, T. Matsui, H. Takehira, T. Taniguchi, M. Koinuma, Y. Matsumoto, T. Akutagawa, T. Nakamura, S. Noro, T. Yamada, H. Kitagawa and S.Hayam, *J. Am. Chem. Soc.*, 2013, **135**, 8097.

55 J. Wootthikanokkhan and N. Seeponkai, *J. Appl. Polym. Sci.*, 2006, **102**, 5941.

56 T. Xu, W. Q. Hou, X. H. Shen, H. Wu, X. C. Li, J. T. Wang and Z. Y. Jiang, *J. Power Sources,* 2011, **196**, 4934.

57 S. Feng, K. Z. Shen, Y. Wang, J. H. Pang and Z. H. Jiang, *J. Power Sources*, 2013, **224**, 42.

58 H. Zhang, H. Ohashi, T. Tamaki and T. Yamaguchi, *J. Phys. Chem. C*, 2013, **117**, 16791.

59 T. Yamaguchi, H. Zhou, S. Nakazawa and N. Hara, *Adv. Mater.*, 2007, **19**, 592.

60 J. Saleem, P. Gao, J. Barford and G. Mckay, *J. Mater. Chem. A,* 2013, **1**, 14335.

61 T. Yamaguchi, F. Miyata and S. Nakao, *Adv. Mater.*, 2003, **15**, 1198.

62 G. W. Li, J. Pan, J. J. Han, C Chen, J. T. Lu and L. Zhuang, *J. Mater. Chem. A,* 2013, **1**, 12497.

63 X. G. Teng, J. C. Dai, J. Su, Y. M. Zhu, H.P. Liu and Z. G. Song, *J. Power Sources*, 2013, **240**, 131.